

Mutual Information Statistics of Optimized LoS MIMO Systems

Michail Matthaiou, Antonios Pitarokoilis, and Josef A. Nossek

Institute for Circuit Theory and Signal Processing, Technische Universität München (TUM),

Arcistrasse 21, 80333, Munich, Germany,

email: {matthaiou, nossek}@nws.ei.tum.de, antonisplit@mytum.de

Abstract—The presence of line-of-sight (LoS) components is typically considered as a hindrance for multiple-input multiple-output (MIMO) communications due to the limited amount of multipath scattering which, in turn, results in low spatial multiplexing gains. However, some recent investigations have questioned this common belief and demonstrated that by employing specifically designed antenna arrays at both the transmitter (Tx) and receiver (Rx), the mean channel matrix can become full-rank and, consequently, we can obtain high channel capacities even at high Ricean K -factors. In this paper, using the joint ordered eigenvalue probability density function (PDF) as a starting point, we derive analytical exact and asymptotic expressions for the mutual information (MI) statistics of these optimized LoS MIMO configurations. The proposed analytical formulae are given in a tractable determinant form and thus can be easily evaluated and efficiently programmed. The implications of the model parameters on MI statistics are also assessed with the match between the analytical curves and Monte-Carlo simulations being excellent.

I. INTRODUCTION

Since their original development by Foschini [1] and Telatar [2], MIMO communication systems have triggered an extensive amount of research and industry interest thanks to their ability to increase channel capacity without sacrificing the operating bandwidth. The great majority of studies reported in literature on MIMO analysis, considers the case of independent and identically (i.i.d.) Rayleigh fading where no LoS path is present and a high number of multipath components is created by the surrounding environment. Under these circumstances, channel capacity can theoretically increase in a linear way with the minimum number of receive and transmit antennas. In practice however, it is very likely that the communications link is dominated by a LoS or specular component; then, the entries of the channel matrix can be more effectively modeled by the Ricean distribution.

Generally speaking, LoS propagation is viewed to limit the beneficial effects of MIMO technology because the channel matrix is normally rank deficient due to the linear dependence of the LoS' rays phases on the receive elements. Hence, the differentiation of the received signals at the MIMO detector becomes difficult due to the reduced multiplexing gain between the different pairs of transmit and receive elements and an unavoidably high percentage of erroneously detected transmitted signals occurs [3], [4]. Over the last years though, research in the field of short-range communications revealed that high capacities are still achievable in LoS by appropriate

positioning of the antenna elements so that the LoS rays become orthogonal [6]–[8].

While these papers provide insightful design methodologies for maximizing LoS MIMO capacity, they do not assess the MI statistics which are critical in the performance evaluation of any MIMO configuration. Recently in [9] and [10], the capacity densities and upper capacity bounds were respectively deduced for dual optimized LoS MIMO systems. In light of this fact, the main goal of the present contribution is to provide a systematic MI characterization for optimized LoS MIMO topologies of *arbitrary size* and with equal LoS eigenvalues. Our analysis relies on the theory of non-central Wishart matrices to derive exact analytical expressions for the MI moment generating function (MGF) and thereafter for its mean and variance. In addition, we provide asymptotic analytical formulae for the MI statistics when the Signal-to-Noise ratio (SNR) goes to infinity. It is worth mentioning that a similar framework was originally proposed in [5] for the case of distinct LoS eigenvalues; yet, the final results were given in integral form containing hypergeometric functions and therefore can be evaluated only numerically.

The remainder of the paper is organized as follows: In Section II, the MIMO channel model used throughout the paper is introduced while Section III elaborates on the properties of non-central Wishart matrices and on the joint eigenvalue PDF for the limiting case of equal LoS eigenvalues. The analytical expressions for the MI statistics are derived in Section IV. A set of numerical results is given in Section V. Finally, Section VI concludes the paper.

Notation: We use upper and lower case boldface to denote matrices and vectors, respectively. The (i, j) -th entry of an $m \times n$ matrix \mathbf{A} is $\{\mathbf{A}\}_{i,j}$ with $1 \leq i \leq m$ and $1 \leq j \leq n$. The symbols $(\bullet)^T$, $(\bullet)^\dagger$ represent the transpose and Hermitian transpose respectively, $\text{tr}(\bullet)$ yields the matrix trace, $\text{etr}(\bullet)$ is shorthand for $\exp(\text{tr}(\bullet))$, and $|\bullet|$ denotes the determinant.

II. MIMO CHANNEL MODEL AND JOINT EIGENVALUE

In the following, we consider a MIMO system equipped with N_t transmit and N_r receive antennas respectively and also define $s \triangleq \min(N_t, N_r)$ and $t \triangleq \max(N_t, N_r)$. In the case of flat Ricean fading, the channel matrix, $\mathbf{H} \in \mathbb{C}^{N_r \times N_t}$, can be modeled as follows

$$\mathbf{H} = \sqrt{\frac{K}{K+1}} \mathbf{H}_L + \sqrt{\frac{1}{K+1}} \mathbf{H}_w \quad (1)$$

where K is the Ricean K -factor expressing the ratio of powers of the free-space signal and the scattered waves. The random component, \mathbf{H}_w , accounts for the scattered signals with its entries being commonly modeled as i.i.d. $\sim \mathcal{CN}(0, 1)$ random variables (Rayleigh fading), while \mathbf{H}_L represents the deterministic non-fading component. As was previously mentioned, in this paper we are particularly interested in optimized full-rank LoS configurations which can be realized by placing the antenna elements sufficiently far apart so that the spatial LoS responses become unique with a phase difference of $\pi/2$ [6]–[8], [11]. We highlight the fact that these configurations are expected to be employed in a plethora of practical applications, such as indoor WLANs, short-range, peer-to-peer and vehicular communications [7], [8], [11].

For the case of parallel arrays¹, the optimum inter-element spacings at the Tx (s_1) and Rx (s_2) have to satisfy the following criterion [7, Eq. (11)], [8, Eq. (28)]

$$s_1 s_2 \approx \lambda D \left(\frac{1}{t} + r \right), \quad r \in \mathbf{Z}^+ \quad (2)$$

where λ is the carrier wavelength and D is the distance between the Tx and Rx.

III. NON-CENTRAL WISHART MATRICES AND JOINT EIGENVALUE PDF

It is evident from (1), that \mathbf{H} has a non-zero mean, given by $E\{\mathbf{H}\} = \mathbf{M} = \sqrt{K/(K+1)}\mathbf{H}_L$ while its correlation matrix reads as $\mathbf{\Sigma} = \varepsilon^2 \mathbf{I}_s$, with $\varepsilon = 1/\sqrt{K+1}$. Moreover, the instantaneous MIMO correlation matrix is defined as

$$\mathbf{W} \triangleq \begin{cases} \mathbf{H}\mathbf{H}^\dagger, & \text{if } N_r \leq N_t \\ \mathbf{H}^\dagger \mathbf{H}, & \text{if } N_r > N_t. \end{cases} \quad (3)$$

We recall that in the case of Ricean fading, $\mathbf{W} \in \mathbb{C}^{s \times s}$ follows an uncorrelated non-central Wishart distribution with t degrees of freedom, i.e. $\mathbf{W} \sim \mathcal{CW}_s(t, \varepsilon^2 \mathbf{I}_s, \mathbf{\Omega})$, where

$$\mathbf{\Omega} \triangleq \begin{cases} \mathbf{\Sigma}^{-1} \mathbf{M} \mathbf{M}^\dagger, & \text{if } N_r \leq N_t \\ \mathbf{\Sigma}^{-1} \mathbf{M}^\dagger \mathbf{M}, & \text{if } N_r > N_t \end{cases} \quad (4)$$

is the non-centrality matrix. Please note that henceforth we will consider a scaled version of \mathbf{W} , that is $\mathbf{S} = \mathbf{\Sigma}^{-1} \mathbf{W} \sim \mathcal{CW}_s(t, \mathbf{I}_s, \mathbf{\Omega})$. Let us denote its eigenvalues by the vector $\boldsymbol{\lambda} \triangleq [\lambda_1, \lambda_2, \dots, \lambda_s]^T$, with $\lambda_1 \geq \lambda_2 \dots \geq \lambda_s \geq 0$ and likewise define the eigenvalues of the non-centrality matrix which are concatenated into the vector $\boldsymbol{\omega} \triangleq [\omega_1, \omega_2, \dots, \omega_s]^T$. For the case of optimized LoS MIMO systems, the latter become identical, or $\omega_1 = \omega_2 \dots = \omega_s = \omega = tK$. It is noteworthy that the channel power is always normalized to unity so that the following condition is fulfilled $E[\text{tr}(\mathbf{W})] = N_r N_t$. The next theorem, which will be the stepping stone of our analysis, returns the joint ordered eigenvalue PDF of \mathbf{S} for the limiting case of equal LoS eigenvalues.

¹The case of tilted arrays admits a similar solution but its study is beyond the scope of the paper. The interested readers are referred to [7], [8].

Theorem 1: The joint ordered eigenvalue PDF of the uncorrelated non-central Wishart matrix $\mathbf{S} \sim \mathcal{CW}_s(t, \mathbf{I}_s, \mathbf{\Omega})$ is

$$f(\boldsymbol{\lambda}) = \frac{\text{etr}(-\boldsymbol{\omega})}{\Gamma_s(s)} |\boldsymbol{\Psi}_c(\boldsymbol{\lambda})| |\boldsymbol{\Phi}(\boldsymbol{\lambda})| \prod_{\ell=1}^s \lambda_\ell^{t-s} e^{-\lambda_\ell} \quad (5)$$

where

$$\{\boldsymbol{\Phi}(\mathbf{x})\}_{i,j} = x_j^{s-i}, \quad \{\boldsymbol{\Psi}_c(\mathbf{x})\}_{i,j} = \frac{x_i^{s-j} {}_0F_1(t+1-j; x_i \omega)}{(t-j)!}$$

while $\Gamma_m(n) = \prod_{i=1}^m (n-i)!$ and ${}_0F_1(\cdot; \cdot)$ denotes the standard generalized hypergeometric function [12, Eq. (9.14.1)].

Proof: A detailed proof is given in Appendix A. ■

IV. MI MGF AND STATISTICS

In [5], it was assumed that the Rx has exact channel state information (CSI) while the Tx knows neither the statistics nor the instantaneous CSI; then, a sensible choice for the Tx is to split the total amount of power equally amongst all data streams (or the uniform power allocation); the authors justify their choice via the so-called 'max-min' property which is a robust transmission scheme to maximize MIMO capacity, when the Tx has no CSI [13]. While this approach simplifies the overall analysis is in general suboptimal especially when the mean channel matrix is rank-deficient [14], [15]. The badness of an isotropic input for arbitrary Ricean channels was quantified in [16], where it was demonstrated that isotropic input is asymptotically optimal only when $N_t \geq N_r$ and for infinitely high SNR.

For the case of optimized LoS configurations with equal LoS eigenvalues, however, isotropic input was shown to be capacity achieving even when the Tx knows the channel statistics [15, Proposition 1]. Based on this key observation, the MI, $I(\mathbf{H})$, can be written as [1], [2]

$$I(\mathbf{H}) = \log_2 \det \left(\mathbf{I}_{N_r} + \frac{\rho}{N_t} \mathbf{H}\mathbf{H}^\dagger \right) = \sum_{\ell=1}^s \log_2 (1 + \rho_c \lambda_\ell)$$

where we have assumed $N_t \geq N_r$, $\rho_c = \rho \varepsilon^2 / N_t$ is the normalized SNR per transmitting antenna with ρ being the SNR as physically measured at each receive antenna. If the channel is ergodic, it suffices to investigate the MI first-order statistics. We can now define the MI MGF according to

$$G(\nu) = E[\exp(\nu I(\mathbf{H}))] = E \left[\prod_{\ell=1}^s (1 + \rho_c \lambda_\ell)^{\frac{\nu}{\ln 2}} \right] \quad (6)$$

with $\text{Re}(\nu) < 0$, while the expectation is taken across all channel realizations of \mathbf{H} .

Theorem 2: The MI MGF of the uncorrelated non-central Wishart matrix $\mathbf{S} \sim \mathcal{CW}_s(t, \mathbf{I}_s, \mathbf{\Omega})$ is equal to

$$G(\nu) = \frac{\text{etr}(-\boldsymbol{\omega})}{\Gamma_s(s)} \det(\boldsymbol{\Lambda}(\nu)) \quad (7)$$

where the entries of the $s \times s$ matrix $\boldsymbol{\Lambda}(\nu)$ are given by

$$\{\boldsymbol{\Lambda}(\nu)\}_{i,j} = \sum_{k=0}^{\infty} \frac{\alpha(k)! \omega^k \rho_c^{-(\alpha(k)+1)}}{k!(t+k-j)!} \times U \left(\alpha(k) + 1, \alpha(k) + 2 + \frac{\nu}{\ln 2}, \frac{1}{\rho_c} \right) \quad (8)$$

with $\alpha(n) = t + s + n - i - j$ and $U(a, b, z)$ denotes the Tricomi confluent hypergeometric function [17, Eq. (13.1.3)].

Proof: The proof starts by invoking the integral definition of the MI MFG, that is

$$G(\nu) = \int_{\mathcal{D}_1} \prod_{\ell=1}^s (1 + \rho_c \lambda_\ell)^{\frac{\nu}{\ln 2}} f(\boldsymbol{\lambda}) d\lambda_1 \dots d\lambda_s \quad (9)$$

where $\mathcal{D}_1 = \{0 < \lambda_1 < \dots < \lambda_s < \infty\}$. Substituting (5) into (9), and using the generic approach of [18, Lemma 1], [5, Appendix B] for the multilinear property of a determinant, we can reach the final result after some algebra and with the aid of the following integral identity [12, Eq. (3.383.5)]

$$\int_0^\infty e^{-\mu y} (1 + \alpha y)^{-n} y^{m-1} dy = \frac{\Gamma(m)}{\alpha^m} U(m, m+1-n, \mu/\alpha).$$

Corollary 1: The MI MGF of $\mathbf{S} \sim \mathcal{CW}_s(t, \mathbf{I}_s, \boldsymbol{\Omega})$ at high-SNRs ($\rho \rightarrow \infty$) is obtained as follows

$$G_{\text{hsnr}}(\nu) = \frac{\text{etr}(-\boldsymbol{\omega}) \rho_c^{s\nu/\ln 2}}{\Gamma_s(s)} \det(\boldsymbol{\Lambda}_{\text{hsnr}}(\nu)) \quad (10)$$

where the entries of the $s \times s$ matrix $\boldsymbol{\Lambda}_{\text{hsnr}}(\nu)$ are given by

$$\{\boldsymbol{\Lambda}_{\text{hsnr}}(\nu)\}_{i,j} = \sum_{k=0}^{\infty} \frac{\omega^k \Gamma(\alpha(k) + 1 + \frac{\nu}{\ln 2})}{k!(t+k-j)!} \quad (11)$$

where $\Gamma(x)$ is the well-known Gamma function.

Proof: The proof stems from Theorem 2 by taking ρ large and performing some basic algebraic manipulations. ■

We emphasize the fact that both (7) and (10) can be efficiently evaluated whereas the similar expression for the case of distinct eigenvalues requires the numerical integration of hypergeometric function (see [5, Eq. (19)]). Moreover, it can be shown that both infinite series yield a fast convergence rate, for all practical values of K and t , and therefore can be truncated to a finite number of terms [19]. The following theorem returns the mean MI (ergodic capacity) of optimized LoS MIMO systems and constitutes the key contribution of the paper.

Theorem 3: The mean MI (ergodic capacity) of the uncorrelated non-central Wishart matrix $\mathbf{S} \sim \mathcal{CW}_s(t, \mathbf{I}_s, \boldsymbol{\Omega})$ is

$$C = E[I(\mathbf{H})] = \frac{\text{etr}(-\boldsymbol{\omega}) e^{1/\rho_c}}{\ln(2) \Gamma_s(s)} \sum_{\ell=1}^s \det(\boldsymbol{\Lambda}_c(\ell)) \quad (12)$$

where the entries of the $s \times s$ matrix $\boldsymbol{\Lambda}_c(\ell)$ are

$$\{\boldsymbol{\Lambda}_c(\ell)\}_{i,j} = \begin{cases} \sum_{k=0}^{\infty} \frac{\alpha(k)! \omega^k \Delta_1(\alpha(k) + 1, \rho_c)}{k!(t+k-j)!}, & j = \ell \\ (t+s-i-j)!/(t-j)! \\ \times {}_1F_1(t+s-i-j+1; t-j+1; \omega), & j \neq \ell \end{cases} \quad (13)$$

where ${}_1F_1(\cdot; \cdot; \cdot)$ is the confluent hypergeometric function [12, Eq. (9.210.1)] and

$$\begin{aligned} \Delta_1(m, \beta) &= \sum_{i=1}^m \frac{\Gamma(-m+i, 1/\beta)}{\beta^{m-i}} \\ &= \sum_{i=0}^{m-1} \mathbb{E}_{i+1}(1/\beta) \end{aligned} \quad (14)$$

with $\Gamma(m, x) = \int_x^\infty t^{m-1} e^{-t} dt$ representing the upper incomplete gamma function [12, Eq. (8.350.2)] while $\mathbb{E}_n(z) = \int_1^\infty e^{-zx} x^{-n} dx$, $n = 0, 1, 2, \dots$, $\text{Re}(z) > 0$ is the exponential integral function of order n [17, Eq. (5.1.4)].

Proof: The proof is based on the definition of the n -th order moment of MI, or

$$E[I(\mathbf{H})^n] = \left. \frac{d^n(G(\nu))}{d\nu^n} \right|_{\nu=0}. \quad (15)$$

Setting $n = 1$ in (15), and using the product rule for the derivative of a determinant in (8), we can obtain the desired result after introducing the Dominated Convergence Theorem to interchange the order of integration and differentiation, and with the aid of [5, Eq. (40)]. ■

Corollary 2: The mean MI (ergodic capacity) of the uncorrelated non-central Wishart matrix $\mathbf{S} \sim \mathcal{CW}_s(t, \mathbf{I}_s, \boldsymbol{\Omega})$ at high SNRs ($\rho \rightarrow \infty$) is

$$C_{\text{hsnr}} = \frac{\text{etr}(-\boldsymbol{\omega})}{\ln(2) \Gamma_s(s)} \sum_{\ell=1}^s \det(\boldsymbol{\Lambda}_{c,\text{hsnr}}(\ell)) \quad (16)$$

with the entries of the $s \times s$ matrix $\boldsymbol{\Lambda}_{c,\text{hsnr}}$ being

$$\{\boldsymbol{\Lambda}_{c,\text{hsnr}}(\ell)\}_{i,j} = \begin{cases} \sum_{k=0}^{\infty} \frac{\alpha(k)! \omega^k}{k!(t+k-j)!} \\ \times (\ln(\rho_c) + \psi(\alpha(k) + 1)), & j = \ell \\ (t+s-i-j)!/(t-j)! \\ \times {}_1F_1(t+s-i-j+1; t-j+1; \omega), & j \neq \ell \end{cases}$$

where $\psi(x)$ is the digamma function [12, Eq. (8.360.1)].

Proof: The proof follows by taking ρ large in (12)–(13) and making use of the integral identity [12, Eq. (4.352.1)]

$$\int_0^\infty x^{m-1} e^{-\mu x} \ln x dx = \mu^{-m} \Gamma(m) (\psi(m) - \ln \mu).$$

The following theorem returns the second MI moment, $E[I(\mathbf{H})^2]$, through which we can obtain the variance of the MI, according to

$$\text{Var}(I(\mathbf{H})) = E[I(\mathbf{H})^2] - (E[I(\mathbf{H})])^2. \quad (17)$$

Theorem 4: The second MI moment of the uncorrelated non-central Wishart matrix $\mathbf{S} \sim \mathcal{CW}_s(t, \mathbf{I}_s, \boldsymbol{\Omega})$ is

$$E[I(\mathbf{H})^2] = \frac{\text{etr}(-\boldsymbol{\omega})}{\ln^2(2) \Gamma_s(s)} \sum_{\ell=1}^s \sum_{n=1}^s \det(\boldsymbol{\Lambda}_v(\ell, n)) \quad (18)$$

where the entries of the $s \times s$ matrix $\boldsymbol{\Lambda}_v(\ell, n)$ are given in (19) at the top of next page while

$$\Delta_2(m, b) = \int_0^\infty y^{m-1} \ln^2(1+by) e^{-y} dy. \quad (20)$$

$$\{\mathbf{\Lambda}_v(\ell, n)\}_{i,j} = \begin{cases} \sum_{k=0}^{\infty} \frac{\omega^k \Delta_2(\alpha(k) + 1, \gamma_c)}{k!(t+k-j)!}, & j = \ell = n \\ \sum_{k=0}^{\infty} \frac{\alpha(k)! \omega^k \Delta_1(\alpha(k) + 1, \gamma_c)}{k!(t+k-j)!}, & j = \ell \text{ or } j = n, \ell \neq n \\ (t+s-i-j)! {}_1F_1(t+s-i-j+1; t-j+1; \omega)/(t-j), & j \neq \ell, j \neq n \end{cases} \quad (19)$$

We note that the integral in (20) admits a closed-form solution by means of Meijer's G -functions according to [5, Eq. (41)] or via a mixture of hypergeometric/exponential integral functions as given in [20, Eq. (20)].

Proof: The proof follows a similar reasoning as in Theorem 3, by simply setting $n = 2$ in (15) and using the known properties for the second-order derivatives of determinants. ■

Evidently, the high-SNR approximation for $E[I(\mathbf{H})^2]$ follows directly by taking ρ infinitely large in (18). Due to space constraints, however, the corresponding relationship is relegated in an extended journal version of this paper [19].

V. NUMERICAL RESULTS

In this section, the theoretical results presented in Section IV are validated via Monte-Carlo simulations. In order to model the optimum LoS configuration, we set the carrier frequency at 5.2 GHz ($\lambda = 5.77$ cm) and the terminal distance at $D = 5$ m. Then using the solution of equal inter-element distances in (2) (for $r = 0$) it is trivial to see that the optimum spacings become $s_1 = s_2 \approx 0.537/\sqrt{t}$. As a next step, 20,000 random realizations of the channel matrix \mathbf{H} are generated according to (1) for each K -factor under consideration.

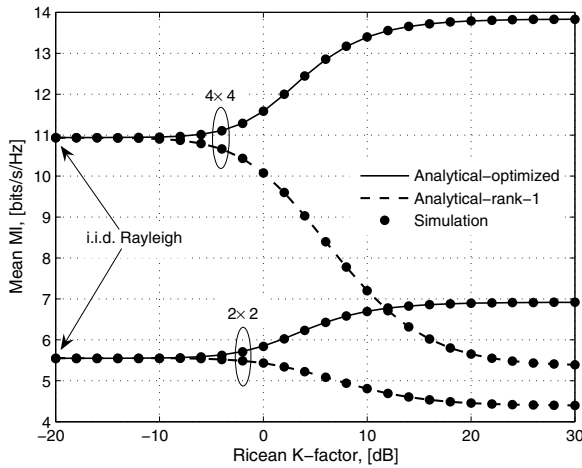


Fig. 1. Mean MI of optimized and conventional MIMO configurations against the Ricean K -factor ($\rho = 10$ dB).

In the first part of the evaluation process, we investigate the effects of deterministic components on the mean MI. In order to get a better understanding, our analysis also considers a conventional rank-1 mean channel matrix which is realized with inter-element spacings of $s_1 = s_2 = \lambda/2 = 2.88$ cm. In Fig. 1,

the ergodic capacity is depicted against the K -factor for two MIMO configurations assuming both optimized/conventional structures for the mean channel matrix ($\rho = 10$ dB). The theoretical curves are based on Theorem 3 for the former case and on [5, Eq. (37)] for the latter.

It is easily seen that the match between theory and simulation is excellent in all cases, thereby validating the correctness of the proposed analytical expressions. The graph contradicts the common belief that the presence of LoS components reduces the advantages of MIMO technology due to limited amount of scattering, compared to Rayleigh fading conditions. As K gets higher, optimized configurations offer the maximum MIMO capacity, i.e. $C_{max} = N_r \log_2(1 + \rho)$, while conventional configurations degenerate into a single-path link, thereby delivering a capacity equal to that of a single-input multiple-output (SIMO) system, i.e. $C_{min} = \log_2(1 + N_r \rho)$. On the other hand, for $K \leq 0$ dB the advantages of optimized configurations diminish and in the limit, $K \rightarrow -\infty$ dB, the LoS component vanishes and we end up with a pure i.i.d. Rayleigh channel.

In Fig. 2, the mean MI is depicted vs the transmit SNR, ρ , for a given $K = 3$ dB and three different MIMO setups. The outputs of a Monte-Carlo simulator are compared with the exact and asymptotic high-SNR expressions of Theorem 3 and Corollary 2, respectively.

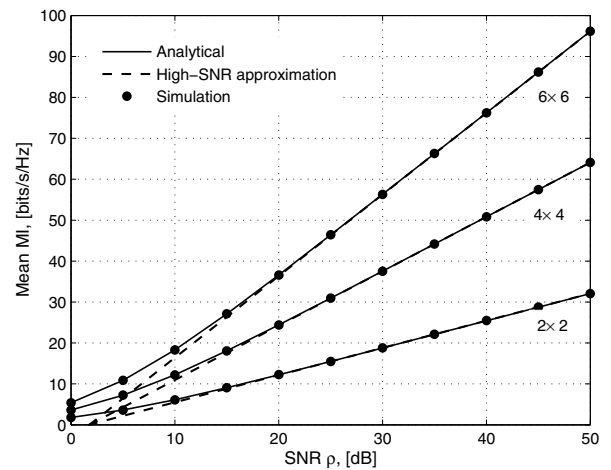


Fig. 2. Mean MI of optimized MIMO configurations against the SNR, ρ ($K = 3$ dB).

Once more, there is an exact agreement between the analytical curves and the Monte-Carlo simulations; further, the

high-SNR expressions seem to become sufficiently tight at $\rho \geq 15$ dB. This implies that they can explicitly predict the mean MI for most practical SNR values with a much lower computational cost.

VI. CONCLUSION

Optimized LoS MIMO configurations are of high practical importance thanks to their inherent ability to deliver high data-rates at any given K -factor. This is achieved by appropriately positioning the antenna elements at both ends, so that sub-channel orthogonality, which is a key condition for capacity maximization, is established. In this paper, we have presented a detailed statistical MI characterization using elements of random matrix theory. The starting point of our analysis has been the joint ordered eigenvalue PDF through which we were able to investigate the MI MGF and its first-order statistics. The derived expressions were validated via numerical simulations and tested under different model parameters, with the attained accuracy being excellent in all cases. All the presented results are given in a tractable determinant form and thus can be evaluated in a straightforward manner.

APPENDIX A PROOF OF THEOREM 1

The proof relies on the joint eigenvalue PDF for the case of distinct eigenvalues, which was originally given by James in [21] and manipulated into a more tractable determinant form by Kang and Alouini in [5]. In particular, we have that

$$f(\lambda) = \frac{\text{etr}(-\omega)}{((t-s)!)^s |\Phi(\omega)|} |\Psi(\lambda)| |\Phi(\lambda)| \prod_{\ell=1}^s \lambda_{\ell}^{t-s} e^{-\lambda_{\ell}} \quad (21)$$

where

$$\{\Psi(\mathbf{x})\}_{i,j} = {}_0F_1(t-s+1; x_i \omega_j) \quad (22)$$

When the LoS eigenvalues coincide, the above equation contains a term of the form

$$\lim_{\omega_1=\omega_2=\dots=\omega_s=\omega} \frac{|{}_0F_1(t-s+1; \lambda_i \omega_j)|}{\prod_{i<j}^s (\omega_i - \omega_j)}. \quad (23)$$

To evaluate these determinant limits we employ the technique proposed by Chiani *et al.* in [22, Lemma 2]. Please note that a similar approach was adopted by Jin *et al.* in [23] as well, for the case of rank- L ($L \leq s$) non-centrality matrices with distinct eigenvalues. In particular, we successively apply the Cauchy's Mean Value Theorem and as such we take the $(s-j)$ -th derivative across the j -th column, evaluated at $\omega_j = \omega$, or

$$\begin{aligned} \lim_{\omega_1=\omega_2=\dots=\omega_s=\omega} \frac{|\Psi(\lambda)|}{|\Phi(\omega)|} &= \frac{\left| \frac{d^{s-j}}{d\omega^{s-j}} {}_0F_1(t-s+1; \lambda_i \omega) \right|}{\Gamma_s(s)} \\ &= \frac{((t-s)!)^s}{\Gamma_s(s)} \left| \sum_{k=0}^{\infty} \frac{\omega^k \lambda_i^{k+s-j}}{k!(t+k-j)!} \right| \end{aligned}$$

where for the differentiation of ${}_0F_1(\alpha; x)$ we have used [17, Eq. (15.2.2)] while the scaling factor $\Gamma_s(s)$ essentially indicates the multiplicity of the LoS eigenvalues [22]. This concludes the proof.

REFERENCES

- [1] G. J. Foschini, "Layered space-time architecture for wireless communications in a fading environment when using multiple antennas," *Bell Labs Tech. Jour.*, vol. 1, no. 2, pp. 41–59, Autumn 1996.
- [2] I. E. Telatar, "Capacity of multi-antenna Gaussian channels," *Europ. Trans. Telecommun.*, vol. 10, no. 6, pp. 585–595, Nov./Dec. 1999.
- [3] L. Cottarelli and M. Debbah, "On the capacity of MIMO Rice channels," in *Proc. Allerton Conference*, IL, 2004.
- [4] —, "The effect of line of sight on the asymptotic capacity of MIMO systems," in *Proc. IEEE Int. Symp. Inf. Theory (ISIT)*, Chicago, IL, June 2004, p. 242.
- [5] M. Kang and M. -S. Alouini, "Capacity of MIMO Rician channels," *IEEE Trans. Wireless Commun.*, vol. 5, no. 1, pp. 112–122, Jan. 2006.
- [6] F. Bøghagen, P. Orten, and G. E. Øien, "Construction and capacity analysis of high-rank line-of-sight MIMO channels," in *Proc. IEEE Wireless Commun. Networking Conf. (WCNC)*, New Orleans, NV, Mar. 2005, pp. 432–437.
- [7] I. Sarris and A. R. Nix, "Design and performance assessment of maximum capacity MIMO architectures in line-of-sight," *IEE Proc. Commun.*, vol. 153, no. 4, pp. 482–488, Aug. 2006.
- [8] —, "Design and performance assessment of high-capacity MIMO architectures in the presence of a line-of-sight component," *IEEE Trans. Veh. Technol.*, vol. 56, no. 4, pp. 2194–2202, July 2007.
- [9] F. Bøghagen, P. Orten, G. E. Øien, and S. de la Kethulle de Ryhove, "Exact capacity expressions for dual-branch Rician MIMO systems," *IEEE Trans. Commun.*, vol. 56, no. 12, pp. 2214–2222, Dec. 2008.
- [10] M. Matthaiou, Y. Kopsinis, D. I. Laurenson, and A. M. Sayeed, "Upper bound for the ergodic capacity of dual MIMO Rician systems: Simplified derivation and asymptotic tightness," *IEEE Trans. Commun.*, vol. 57, no. 12, pp. 3589–3596, Dec. 2009.
- [11] M. Matthaiou, D. I. Laurenson, and C. -X. Wang, "Capacity study of vehicle-to-roadside MIMO channels with a line-of-sight component," in *Proc. IEEE Wireless Commun. Networking Conf. (WCNC)*, Las Vegas, NV, Mar. 2008, pp. 775–779.
- [12] I. S. Gradshteyn and I. M. Ryzhik, *Table of Integrals, Series, and Products*, Seventh Ed. Academic Press, San Diego, 2007.
- [13] H. Boche and E. Jorswieck, "On the ergodic capacity as a function of the correlation properties in systems with multiple transmit antennas without CSI at the transmitter," *IEEE Trans. Commun.*, vol. 52, no. 10, pp. 1654–1657, Oct. 2004.
- [14] D. Höslı and A. Lapidoth, "The capacity of a MIMO Rician channel is monotonic in the singular values of the mean," in *Proc. ITG Int. Conf. Source Channel Coding*, Erlangen, Germany, Jan. 2004.
- [15] A. M. Tulino, A. Lozano, and S. Verdú, "Capacity-achieving input covariance for single-user multiantenna channels," *IEEE Trans. Wireless Commun.*, vol. 5, no. 2, pp. 662–671, Mar. 2006.
- [16] D. Höslı and A. Lapidoth, "How good is an isotropic Gaussian input on a MIMO Rician channel?," in *Proc. IEEE Int. Symp. Inf. Theory (ISIT)*, Chicago, IL, Jul. 2004, pp. 291.
- [17] M. Abramowitz and I. A. Stegun, *Handbook of Mathematical Functions with Formulas, Graphs, and Mathematical Tables*, Ninth Ed., NY, Dover, 1970.
- [18] G. G. Khatri, "Non-central distributions of i th largest characteristic roots of three matrices concerning complex multivariate normal populations," *Ann. Inst. Statist. Math.*, vol. 21, no. 1, pp. 23–32, Dec. 1969.
- [19] M. Matthaiou, P. de Kerret, G. K. Karagiannidis, and J. A. Nossek, "Mutual information statistics and beamforming performance analysis of optimized LoS MIMO systems," submitted to *IEEE Trans. Commun.*, Dec. 2009.
- [20] J. Chen and K. -K. Wong, "Power minimization of central Wishart MIMO block-fading channels," *IEEE Trans. Commun.*, vol. 57, no. 4, pp. 899–905, Apr. 2009.
- [21] A. T. James, "Distributions of matrix variates and latent roots derived from normal samples," *Ann. Math. Stat.*, vol. 35, no. 2, pp. 475–501, June 1964.
- [22] M. Chiani, M. Z. Win, and H. Shin, "Capacity of MIMO systems in the presence of interference," in *Proc. IEEE Global Telecommun. Conf. (GLOBECOM)*, San Francisco, CA, Nov. 2006.
- [23] S. Jin, M. R. McKay, X. Gao, and I. B. Collings, "MIMO multichannel beamforming: SER and outage using new eigenvalue distribution of complex noncentral Wishart matrices," *IEEE Trans. Commun.*, vol. 56, no. 3, pp. 424–434, Mar. 2008.